

Cloning and Characterization of Voltage-Gated Calcium Channel Alpha1 Subunits in *Xenopus laevis* During Development

Brittany B. Lewis,[†] Matthew R. Wester,[†] Lauren E. Miller, Maitreyi D. Nagarkar, M. Brittany Johnson,[‡] and Margaret S. Saha*

Voltage-gated calcium channels play a critical role in regulating the Ca^{2+} activity that mediates many aspects of neural development, including neural induction, neurotransmitter phenotype specification, and neurite outgrowth. Using *Xenopus laevis* embryos, we describe the spatial and temporal expression patterns during development of the 10 pore-forming alpha1 subunits that define the channels' kinetic properties. In situ hybridization indicates that $Ca_v1.2$, $Ca_v2.1$, $Ca_v2.2$, and $Ca_v3.2$ are expressed during neurula stages throughout the neural tube. These, along with $Ca_v1.3$ and $Ca_v2.3$, beginning at early tail bud stages, and $Ca_v3.1$ at late tail bud stages, are detected in complex patterns within the brain and spinal cord through swimming tadpole stages. Additional expression of various alpha1 subunits was observed in the cranial ganglia, retina, olfactory epithelium, pineal gland, and heart. The unique expression patterns for the different alpha1 subunits suggests they are under precise spatial and temporal regulation and are serving specific functions during embryonic development. *Developmental Dynamics* 238:2891–2902, 2009. © 2009 Wiley-Liss, Inc.

Key words: *Xenopus*; calcium channel; alpha1 subunit; $Ca_v1.1$; $Ca_v1.2$; $Ca_v1.3$; $Ca_v1.4$; $Ca_v2.1$; $Ca_v2.2$; $Ca_v2.3$; $Ca_v3.1$; $Ca_v3.2$; $Ca_v3.3$; nervous system; embryo

Accepted 21 August 2009

INTRODUCTION

Changes in intracellular Ca^{2+} are responsible for regulating a diverse array of cellular and physiological processes, including release of neurotransmitter and hormone, muscle contraction, chemotaxis, pacemaker activity, synapse formation, and gene expression (Perez-Reyes and Schneider, 1995; Yamakage and Namiki, 2002; Catterall et al., 2005; McKeown et al., 2006; Calin-Jageman and Lee, 2008). While the role of Ca^{2+} fluctuations and their underlying molecular mechanisms are well characterized in

mature cells, Ca^{2+} activity plays an equally important role during development (Borodinsky and Spitzer, 2006; Webb and Miller, 2006). During early embryogenesis, Ca^{2+} fluxes are essential for coordinating cellular events following fertilization (Horner and Wolfner, 2008) and have also been implicated in the regulation of cell division (Li et al., 2008), convergent-extension (Wallingford et al., 2001), and dorsoventral patterning of the mesoderm (Palma et al., 2001). Ca^{2+} activity also regulates virtually every phase of neural development, including the induction of the nervous system (Leclerc

et al., 2006; Webb and Miller, 2006; Moreau et al., 2008), maturation of the potassium current and other electrical properties of the cell (Spitzer and Ribera, 1998; Spitzer et al., 2002), and neurite outgrowth (Conklin et al., 2005). Recent work has shown that the specification of neurotransmitter phenotype is associated with Ca^{2+} activity, with higher frequencies of Ca^{2+} spiking during a critical developmental period linked to the specification of inhibitory phenotypes and lower levels of spiking resulting in excitatory phenotypes (Borodinsky et al., 2004; Spitzer, 2006; Root et al., 2008).

Department of Biology, The College of William and Mary, Integrated Science Center, Williamsburg, Virginia

Grant sponsor: Howard Hughes Medical Institute; Grant number: 52005868.

[†]B.R. Lewis and M.R. Wester contributed equally to this work.

[‡]M.B. Johnson's present address is University of Virginia, Department of Microbiology, Charlottesville, VA 22902.

*Correspondence to: Margaret S. Saha, Department of Biology, Integrated Science Center, Landrum Drive, Williamsburg, VA 23185. E-mail: mssaha@wm.edu

DOI 10.1002/dvdy.22102

Published online 30 September 2009 in Wiley InterScience (www.interscience.wiley.com).

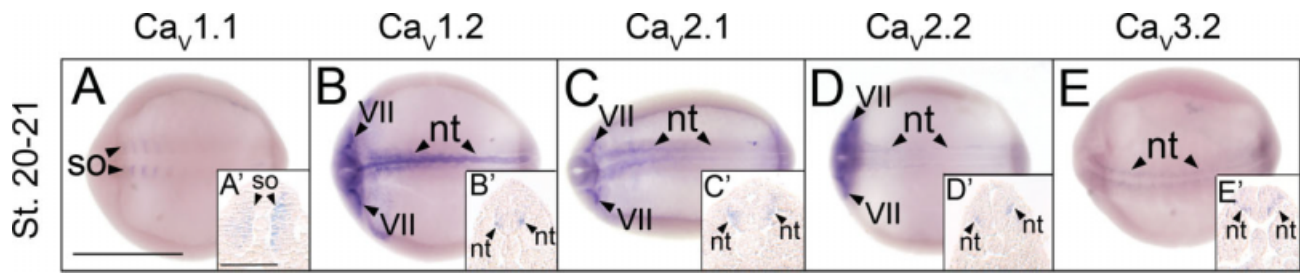


Fig. 1.

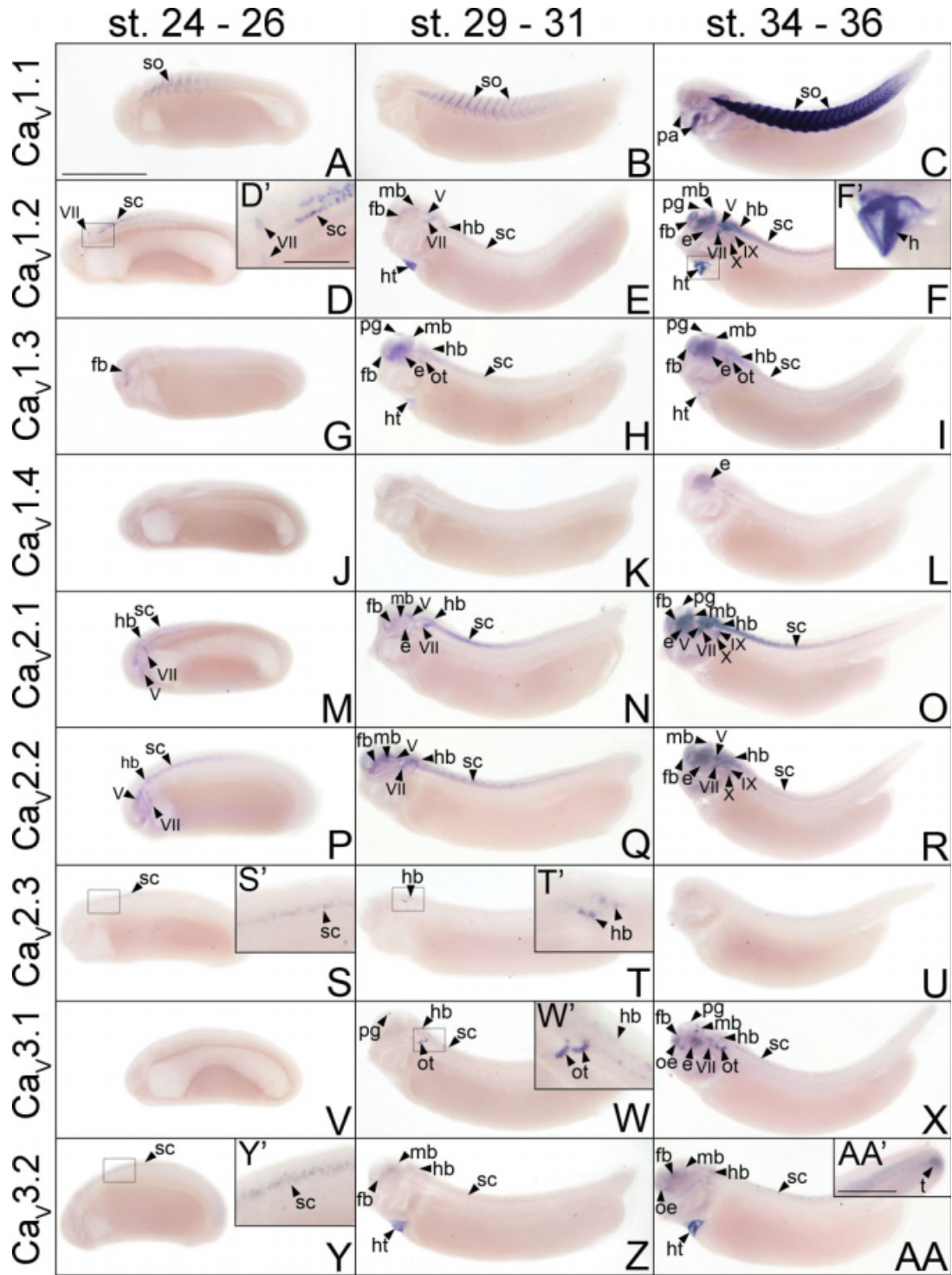


Fig. 2.

The molecular mechanisms governing Ca^{2+} concentrations within cells include a wide array of both intracellular and extracellular channels, pumps, and sensors; the superfamily of voltage-gated calcium channels (VGCCs) plays a particularly critical role in regulating intracellular Ca^{2+} levels both temporally and spatially (Catterall et al., 2005; Kisilevsky and Zamponi, 2008). VGCCs consist of an $\alpha 1$ subunit, which contains the major pore-forming region and voltage sensor and largely determines the channel's physiological characteristics, as well as auxiliary $\alpha 2$ - δ , β , and γ subunits which are able to modulate the channel's properties (Catterall, 2000; Obermair et al., 2008). In vertebrates, 10 different $\alpha 1$ subunits have been identified along with 4 $\alpha 2$ - δ subunits, 4 β subunits, and 2 γ subunits. The expression patterns of many of these subunits have been studied in the adult due to their critical role in regulating the physiology of excitable cells and their growing association with several pathologies (McKeown et al., 2006). Despite the clear importance of the role of VGCCs during development (Spitzer et al., 2005; Leclerc et al., 2006), the expression and function of these channels during embryogenesis is less well investigated. While there are detailed analyses of the β subunits in zebrafish (Zhou et al., 2006, 2008), there are only limited data on selected $\alpha 1$ subunits in zebrafish (Sanhueza et al., 2009) and amphibians (Palma et al., 2001; Jimenez-Gonzalez et al., 2003; Zhou et al., 2006, 2008). In mammals, there are reports describing expression of specific channels in defined tissues, usually for the later stages of embryogenesis (Son et al., 2002; Xu et al., 2003;

Niwa et al., 2004). However, there is currently no comprehensive description of the $\alpha 1$ subunits during vertebrate embryogenesis.

Here, we have chosen to examine the expression patterns of the 10 $\alpha 1$ subunits during embryogenesis in *Xenopus laevis*. The choice of *Xenopus* is particularly suitable given the large size of the eggs, which are accessible at early developmental stages, the ability to conduct embryological manipulations and transgenesis, and the sequenced genome of *X. tropicalis*. Perhaps most importantly, many of the roles for Ca^{2+} activity during embryonic development (e.g., activity dependent neurotransmitter phenotype specification) were first reported in *X. laevis* and continue to be widely studied in this species. Here, we show that the $\alpha 1$ subunits are expressed in complex, unique, and dynamic patterns that are tightly regulated both temporally and spatially, suggesting specific roles for these subunits during vertebrate embryogenesis.

RESULTS

Voltage-Gated Calcium Channel $\alpha 1$ Subunit Sequences

Ten different VGCC $\alpha 1$ subunits corresponding to *Ca_V1.1* (GenBank accession no. GQ120633), *Ca_V1.2* (GQ120626), *Ca_V1.3* (GQ120627), *Ca_V1.4* (GQ120629), *Ca_V2.1* (GQ120624), *Ca_V2.2* (GQ120625), *Ca_V2.3* (GQ120628), *Ca_V3.1* (GQ120630), *Ca_V3.2* (GQ120631), and *Ca_V3.3* (GQ120632) were cloned from *X. laevis* cDNA using reverse transcriptase-polymerase chain reaction (RT-PCR). In all cases, BLAST N

and BLAST X searches confirmed the identity of the cloned subunit with E values consistently less than 6.0×10^{-25} for BLAST N and 5.0×10^{-51} for BLAST X.

Early Expression of *Ca_V1.1*, *Ca_V1.2*, *Ca_V2.1*, *Ca_V2.2*, and *Ca_V3.2*

The first subunits to be detected in the developing *X. laevis* embryo are *Ca_V1.1*, *Ca_V1.2*, *Ca_V2.1*, *Ca_V2.2*, and *Ca_V3.2*. Transcripts for these subunits are observed beginning at neurula stages. With the exception of *Ca_V1.1*, which is expressed in the somites (Fig. 1A,A'), these subunits are all expressed in the neural tube (Fig. 1B–E,B'–E'). Transcripts for *Ca_V1.2*, *Ca_V2.1*, and *Ca_V2.2* are also detected in cranial placode VII (Fig. 1B–D).

Expression of *Ca_V1.2*, *Ca_V1.3*, *Ca_V2.1*, *Ca_V2.2*, *Ca_V3.1*, and *Ca_V3.2* in the Forebrain

By swimming tadpole stages of development, the VGCC $\alpha 1$ subunits *Ca_V1.2*, *Ca_V1.3*, *Ca_V2.1*, *Ca_V2.2*, *Ca_V3.1*, and *Ca_V3.2* are all expressed in discrete patterns throughout the forebrain. *Ca_V1.3* is the first transcript to be detected at early tail bud stages in the diencephalon (Fig. 2G). This expression spreads to the telencephalon and pineal gland by late tail bud stages (Fig. 2H) and persists into swimming tadpole stages (Fig. 2I). Expression of *Ca_V1.3* at these stages is most prominent in the pineal gland, but transcripts can be detected at low levels throughout the forebrain, particularly in the ventral domain (Fig. 3C).

After the initial appearance of *Ca_V1.3* expression, transcripts for *Ca_V1.2*, *Ca_V2.1*, and *Ca_V3.2* are all

Fig. 1. Spatial expression patterns of VGCC $\alpha 1$ subunits in stage 20–21 (neurula) *Xenopus laevis* embryos using whole-mount in situ hybridization. Embryos were viewed dorsally, with anterior to the left. **A,A'**: *Ca_V1.1* expression. **B,B'**: *Ca_V1.2* expression. **C,C'**: *Ca_V2.1* expression. **D,D'**: *Ca_V2.2* expression. **E,E'**: *Ca_V3.2* expression. Arrowheads indicate regions of expression. nt, neural tube; so, somite; VII, cranial placode VII, geniculate (facialis) placode. Scale bar = 1.0 mm in A–E; 0.25 mm in A'–E'.

Fig. 2. Spatial and temporal expression patterns of VGCC $\alpha 1$ subunits in developing *X. laevis* embryos using whole-mount in situ hybridization. Embryos were viewed laterally, with anterior to the left and dorsal to the top. A,D,G,J,M,PS,V,Y: Stages 24–26 (early tail bud). B,E,H,K,N,Q,T,W,Z: Stages 29–31 (late tail bud). C,F,I,L,O,R,U,X,AA: Stages 34–36 (swimming tadpole). **A–C**: *Ca_V1.1* expression. **D–F**: *Ca_V1.2* expression. **G–I**: *Ca_V1.3* expression. **J–L**: *Ca_V1.4* expression. **M–O**: *Ca_V2.1* expression. **P–R**: *Ca_V2.2* expression. **S–U**: *Ca_V2.3* expression. **V–X**: *Ca_V3.1* expression. **Y–AA**: *Ca_V3.2* expression. **D',F',S',T',W',Y'**: Magnified images of portions of the embryos indicated by the hollow boxes. **AA'**: Magnified image of the tail of an embryo at swimming tadpole stage showing *Ca_V3.2* expression. Arrowheads indicate regions of expression. fb, forebrain; e, eye; hb, hindbrain; ht, heart; mb, midbrain; oe, olfactory epithelium; ot, otic vesicle; pa, pharyngeal arches; pg, pineal gland; sc, spinal cord; so, somite; t, tail bud; V, cranial ganglion V, trigeminal ganglion; VII, cranial ganglion VII, geniculate (facialis) ganglion; IX, cranial ganglion IX, glossopharyngeal ganglion; X, cranial ganglion X, vagal ganglion. Scale bars = 1.0 mm in A–AA, 0.4 mm in AA'; 0.2 mm in D',F',S',T',W',Y'.

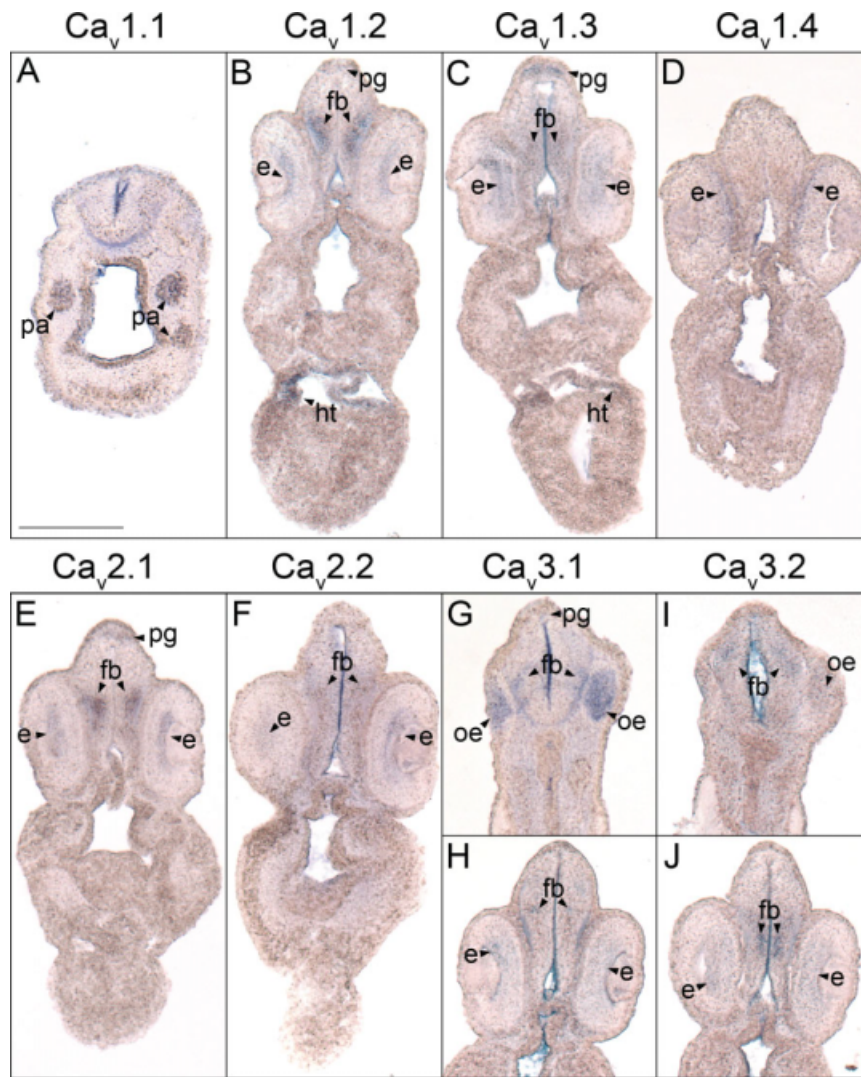


Fig. 3. Forebrain histological analysis of voltage-gated calcium channel (VGCC) $\alpha 1$ subunit expression in stages 35–37 (swimming tadpole) *Xenopus laevis* using whole-mount in situ hybridization. A–J: Transverse 18- μ m sections within the forebrain region of the anterior–posterior axis, with dorsal to the top. **A:** $Ca_V1.1$ expression. **B:** $Ca_V1.2$ expression. **C:** $Ca_V1.3$ expression. **D:** $Ca_V1.4$ expression. **E:** $Ca_V2.1$ expression. **F:** $Ca_V2.2$ expression. **G,H:** $Ca_V3.1$ expression. **I,J:** $Ca_V3.2$ expression. Arrowheads indicate regions of expression. fb, forebrain; e, eye; ht, heart; oe, olfactory epithelium; pa, pharyngeal arches; pg, pineal gland. Scale bar = 0.25 mm.

detected in the diencephalon (Fig. 2E,N,Z) and $Ca_V2.2$ mRNA is observed in both the telencephalon and diencephalon by late tail bud stages of development (Fig. 2Q). Like $Ca_V1.3$, the expression domains of these $\alpha 1$ subunits each expand throughout the forebrain as development progresses to swimming tadpole stages (Fig. 2F,O,R,AA). (Swimming tadpole stages are defined as Nieuwkoop Faber stages 34–36, when the embryo exhibits spontaneous swimming movements and reflexively swims away from adverse stimuli). $Ca_V1.2$ and $Ca_V2.1$ tran-

scripts also appear in the pineal gland, albeit at lower levels than $Ca_V1.3$ (Figs. 2F,O, 3B,E). Within the forebrain, $Ca_V1.2$, $Ca_V2.1$, and $Ca_V2.2$ are all expressed primarily in postmitotic domains (as opposed to domains lining the ventricle) midway along the dorsal–ventral axis (Fig. 3B,E,F). $Ca_V3.2$, however, displays a distinct expression pattern. In the telencephalon, $Ca_V3.2$ transcripts appear in dorsal postmitotic cells (Fig. 3I), while a distinct domain of expression is detected midway along the dorsal–ventral axis in the ventricular layer of the diencephalon (Fig. 3J).

The onset of $Ca_V3.1$ expression coincides with that of $Ca_V1.2$, $Ca_V2.1$, $Ca_V2.2$, and $Ca_V3.2$ in the forebrain at late tail bud stages, but it is initially localized in a discrete region of the pineal gland rather than in the forebrain (Fig. 2W). $Ca_V3.1$ transcripts persist in the pineal gland into swimming tadpole stages, and they appear in a ventral domain of postmitotic cells in the telencephalon and in a small, slightly dorsal postmitotic region of the diencephalon (Figs. 2X, 3G,H).

Expression of $Ca_V1.2$, $Ca_V1.3$, $Ca_V2.1$, $Ca_V2.2$, $Ca_V3.1$, and $Ca_V3.2$ in the Midbrain

The same array of VGCC $\alpha 1$ subunits expressed in the forebrain during embryonic development of *X. laevis* also appears in a range of patterns within the midbrain. Transcripts for $Ca_V1.2$, $Ca_V1.3$, $Ca_V2.1$, $Ca_V2.2$, and $Ca_V3.2$ simultaneously first appear in the midbrain during late tail bud stages (Fig. 2E,H,N,Q,Z). The expression of each of these subunits strengthens in partially overlapping domains throughout development into swimming tadpole stages (Fig. 2F,I,O,R,AA). Expression of $Ca_V1.2$ is restricted to a small ventral region of postmitotic cells within the midbrain (Fig. 4A,B), while $Ca_V1.3$ and $Ca_V2.1$ transcripts are detected in the same region but extend further dorsally (Fig. 4C–E). $Ca_V2.2$ appears to be expressed in an area similar to $Ca_V1.3$ and $Ca_V2.1$ but at much lower levels (Fig. 4F,G). $Ca_V3.2$ mRNA is detected in a slightly more dorsal region than $Ca_V1.2$ but is still contained within the expression domains of $Ca_V1.3$, $Ca_V2.1$, and $Ca_V2.2$ (Fig. 4J).

Unlike the other five $\alpha 1$ subunits, the initial expression of $Ca_V3.1$ in the midbrain is delayed until swimming tadpole stages of development (Fig. 2X). The spatial pattern of expression for this $\alpha 1$ subunit also differs from the others, appearing in three small, distinct regions of postmitotic cells (Figs. 2X, 4H, I). The two anterior domains flank the midline of the dorsal–ventral axis of the midbrain, while the posterior domain is slightly ventral and extends farther laterally (Fig. 4H,I), much like the $Ca_V3.2$ pattern of expression in this region.

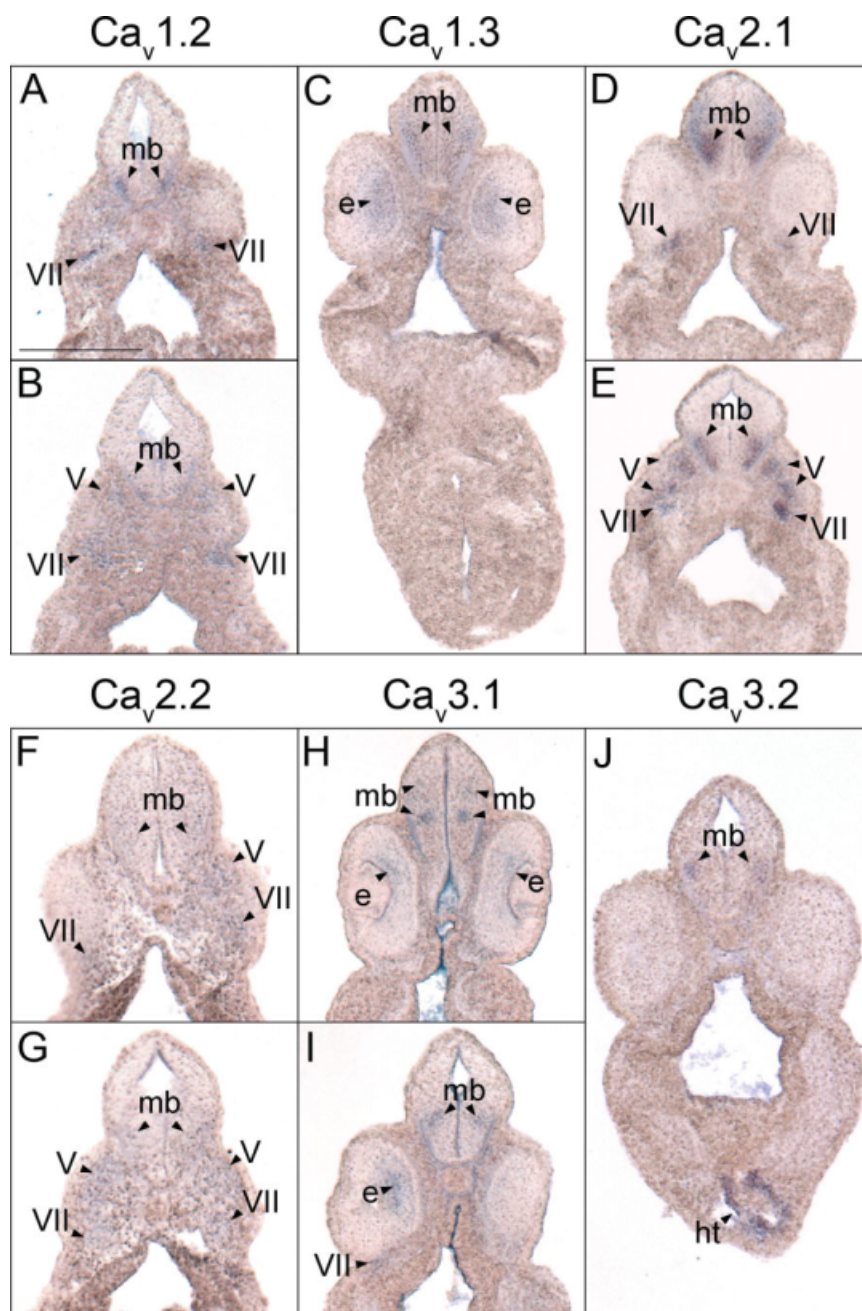


Fig. 4. Midbrain histological analysis of voltage-gated calcium channel (VGCC) α subunit expression in stages 35–37 (swimming tadpole) *X. laevis* using whole-mount in situ hybridization. A–J: Transverse 18- μ m sections within the midbrain region of the anterior–posterior axis, with dorsal to the top. **A,B:** $Ca_v1.2$ expression. **C:** $Ca_v1.3$ expression. **D,E:** $Ca_v2.1$ expression. **F,G:** $Ca_v2.2$ expression. **H,I:** $Ca_v3.1$ expression. **J:** $Ca_v3.2$ expression. Arrowheads indicate regions of expression. mb, midbrain; e, eye; ht, heart; V, cranial ganglion V, trigeminal ganglion; VII, cranial ganglion VII, geniculate (facialis) ganglion. Scale bar = 0.25 mm.

Expression of $Ca_v1.2$, $Ca_v1.3$, $Ca_v2.1$, $Ca_v2.2$, $Ca_v2.3$, $Ca_v3.1$, and $Ca_v3.2$ in the Hindbrain

As in the fore- and midbrain, the VGCC α subunits $Ca_v1.2$, $Ca_v1.3$, $Ca_v2.1$, $Ca_v2.2$, $Ca_v3.1$, and $Ca_v3.2$

are all expressed in the hindbrain during *X. laevis* embryogenesis. The onset of hindbrain expression for $Ca_v2.1$ and $Ca_v2.2$ occurs during early tail bud stages (Fig. 2M,P), while $Ca_v1.2$, $Ca_v1.3$, $Ca_v3.1$, and $Ca_v3.2$ transcripts appear during late tail bud stages (Fig. 2E,H,W,Z).

Expression of each increases in prominence within the hindbrain through swimming tadpole stages (Fig. 2F,I,O,R,X,AA), but in varying spatial patterns. Similar to the midbrain, $Ca_v1.2$ mRNA is expressed in a ventrally restricted domain of postmitotic cells near the anterior portion of the hindbrain (Fig. 5B), but transcripts extend farther dorsally in the posterior hindbrain (Fig. 5C). $Ca_v1.3$, $Ca_v2.2$, and $Ca_v2.1$ are all expressed in a wider ventral region along the entire anterior–posterior range of the hindbrain (Fig. 5D–G). The domains of $Ca_v3.1$ and $Ca_v3.2$ expression are more medial along the dorsal–ventral axis of the hindbrain, with $Ca_v3.1$ mRNA detectable more laterally than $Ca_v3.2$ (Fig. 5J,K). Coincident with hindbrain expression at late tail bud stages, $Ca_v1.3$ and $Ca_v3.1$ appear along the ventral side of the otic vesicle (Fig. 2H,W,W'), where they persist into swimming tadpole stages of development (Figs. 2I,X, 5D,D',J,J').

The α 1 subunit $Ca_v2.3$ is expressed transiently within the hindbrain. Like $Ca_v1.2$, $Ca_v1.3$, $Ca_v3.1$, and $Ca_v3.2$, its onset of expression in this region of the central nervous system (CNS) is during late tail bud stages of development (Fig. 2T,T'), appearing in a small, slightly ventral region of postmitotic cells (Fig. 5I). However, unlike these other α 1 subunits, $Ca_v2.3$ expression is transient, with transcripts disappearing in the hindbrain by swimming tadpole stages (Fig. 2U).

Expression of $Ca_v1.2$, $Ca_v1.3$, $Ca_v2.1$, $Ca_v2.2$, $Ca_v2.3$, $Ca_v3.1$, and $Ca_v3.2$ in the Spinal Cord

The same VGCC α 1 subunits expressed in the hindbrain are also observed in the spinal cord. During neurula stages, transcripts for $Ca_v1.2$, $Ca_v2.1$, $Ca_v2.2$, and $Ca_v3.2$ are all detected in the developing neural tube (Fig. 1B–E,B'–E'). The expression of each of these subunits persists in the spinal cord throughout development into swimming tadpole stages (Fig. 2D–F, D',M–R,Y–AA,Y'). $Ca_v2.3$ expression begins later, during early tail bud stages, but it

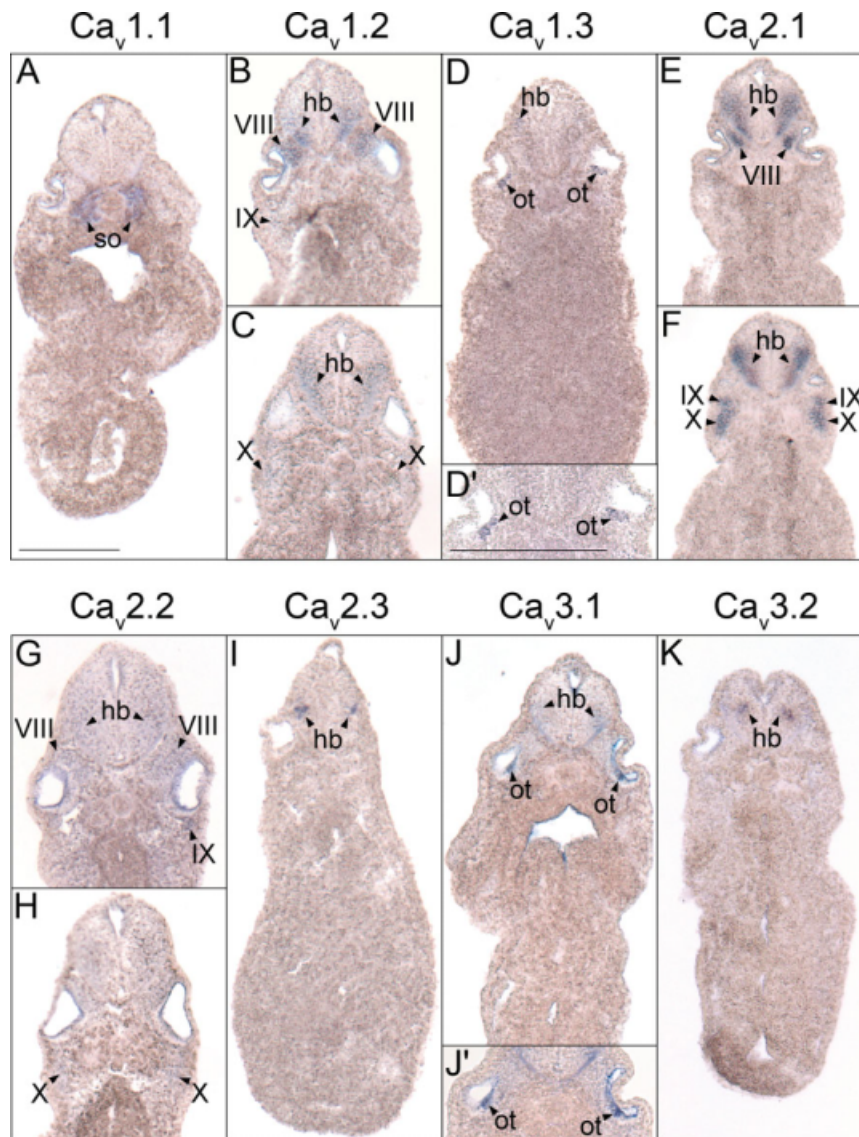


Fig. 5. Hindbrain histological analysis of voltage-gated calcium channel (VGCC) $\alpha 1$ subunit expression in (A–G,J,K) stage 35–37 (swimming tadpole) or (I) stage 30 (late tail bud) *X. laevis* using whole-mount in situ hybridization. A–K: Transverse 18- μ m sections of embryos within the hindbrain region of the anterior–posterior axis, with dorsal to the top. **A:** $Ca_V1.1$ expression. **B,C:** $Ca_V1.2$ expression. **D:** $Ca_V1.3$ expression. **E,F:** $Ca_V2.1$ expression. **G,H:** $Ca_V2.2$ expression. **I:** $Ca_V2.3$ expression. **J:** $Ca_V3.1$ expression. **K:** $Ca_V3.2$ expression. Arrowheads indicate regions of expression. hb, hindbrain; ot, otic vesicle; so, somite; VIII, cranial ganglion VIII, acousticus ganglion; IX, cranial ganglion IX, glossopharyngeal ganglion; X, cranial ganglion X, vagal ganglion. Scale bar represents 0.25 mm.

disappears by late tail bud stages (Fig. 2S,S',T). $Ca_V1.3$ and $Ca_V3.1$ transcripts also appear in the anterior spinal cord beginning at stage 29, and they persist into swimming tadpole stages (Fig. 2H,I,W,X). $Ca_V1.2$ and $Ca_V2.1$ are expressed most prominently in the ventral half of the postmitotic domain of the spinal cord (Fig. 6B,D), while $Ca_V1.3$ and $Ca_V2.2$ are expressed in the same region along the dorsal–ventral axis but more pos-

teriorly (Fig. 6C,E). $Ca_V1.3$ mRNA also appears restricted to the anterior spinal cord (Fig. 2I). $Ca_V3.1$ and $Ca_V3.2$ are expressed in smaller postmitotic regions that are more medial along the dorsal–ventral axis of the spinal cord than the other $\alpha 1$ subunits (Fig. 6F,G). Finally, unlike the other subunits, $Ca_V3.2$ is expressed in a small area at the tip of the tail bud during swimming tadpole stages (Fig. 2AA').

Expression of $Ca_V1.2$, $Ca_V2.1$, $Ca_V2.2$, and $Ca_V3.1$ in the Cranial Ganglia

The VGCC $\alpha 1$ subunits $Ca_V1.2$, $Ca_V2.1$, $Ca_V2.2$, and $Ca_V3.1$ are expressed at different times and in various combinations in the cranial ganglia and their developmental precursors, the cranial placodes, of *X. laevis*. $Ca_V1.2$, $Ca_V2.1$, and $Ca_V2.2$ transcripts are all detected in cranial placode VII beginning at neurula stages (Fig. 1B–D). While $Ca_V2.1$ and $Ca_V2.2$ continue to be expressed in cranial placode VII and appear in cranial placode V during early tail bud stages (Fig. 2M,P), $Ca_V1.2$ mRNA remains detectable only in cranial placode VII (Fig. 2D). By late tail bud stages, $Ca_V1.2$ transcripts appear in cranial ganglion V (Fig. 2E) but at lower levels than $Ca_V2.1$ and $Ca_V2.2$ (Fig. 2N,Q). The expression of each of these subunits persists in cranial ganglia V and VII and is also observed in cranial ganglia VIII, IX, and X as well in swimming tadpole stages (Figs. 2F,O,R, 4A,B,D–G, 5B,C,E–G). At this time, cranial ganglion VII also begins to express $Ca_V3.1$ (Figs. 2X, 4I). Expression of $Ca_V3.1$ and, to a much lesser degree, $Ca_V3.2$ are observed in the olfactory epithelium by swimming tadpole stages of development (Figs. 2X,AA, 3G,I). No VGCC $\alpha 1$ subunit transcripts are detected in presumptive cranial nerves II, III, or XI.

Expression of $Ca_V1.2$, $Ca_V1.3$, $Ca_V1.4$, $Ca_V2.1$, $Ca_V2.2$, $Ca_V3.1$, and $Ca_V3.2$ in the Retina

With the exception of $Ca_V2.3$, all of the VGCC $\alpha 1$ subunits that are expressed in the *X. laevis* embryonic brain and spinal cord are also detected in the developing retina. $Ca_V1.3$ and $Ca_V2.1$ are the first transcripts to appear at low levels in the retina during late tail bud stages (Fig. 2H,N), but by swimming tadpole stages, expression of $Ca_V1.2$, $Ca_V1.3$, $Ca_V2.1$, $Ca_V2.2$, $Ca_V3.1$, and $Ca_V3.2$ is observed (Fig. 2F,I,O,R,X,AA). Expression of $Ca_V1.4$, which is not observed in any region of the embryo before this stage, also appears in the retina (Fig. 2L). $Ca_V1.2$, $Ca_V2.1$, and

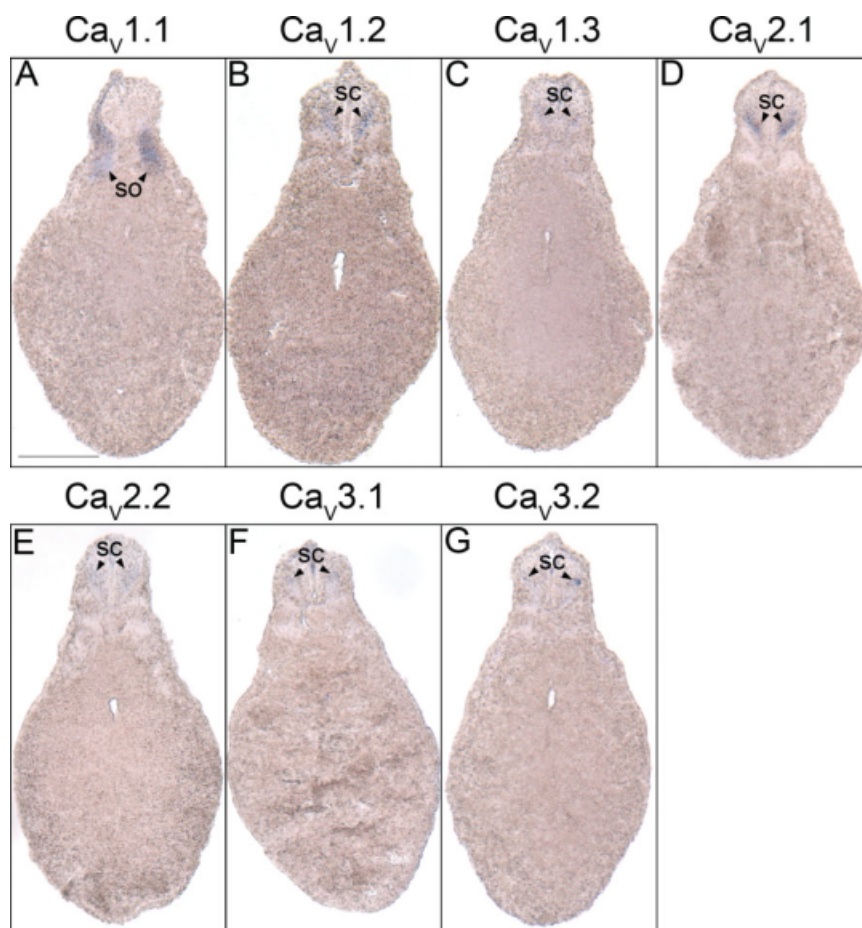


Fig. 6.

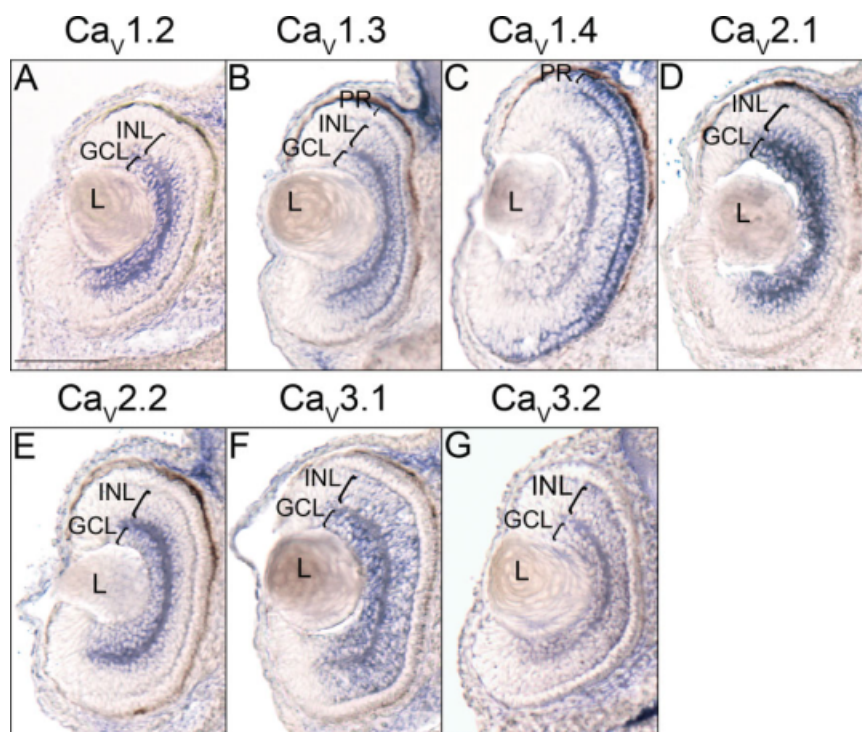


Fig. 7.

$Ca_{v2.2}$ all appear to be expressed in layers in the central retina (Fig. 3B,E,F); histological analysis of embryos at stage 40 shows transcripts for these subunits to be expressed in the ganglion cell layer (GCL) and the inner portion of the inner nuclear layer (INL; Fig. 7A,D,E). $Ca_{v1.3}$, $Ca_{v3.1}$, and to a lesser extent $Ca_{v3.2}$ are expressed in a wider area of the retina (Fig. 3C,H,J), and appear later, at stage 40, to encompass all of the GCL and INL (Fig. 7B,F,G). $Ca_{v1.4}$ is expressed in a narrow outer layer of the retina (Fig. 3D), which analysis at stage 40 identifies as photoreceptor cells (PR; Fig. 7C). $Ca_{v1.3}$ expression is also observed at low levels in the PR at this later stage (Fig. 7B).

Expression of $Ca_{v1.2}$, $Ca_{v1.3}$, and $Ca_{v3.2}$ in the Heart

Beginning at late tail bud stages, the VGCC $\alpha 1$ subunits $Ca_{v1.2}$, $Ca_{v1.3}$, and $Ca_{v3.2}$ are all expressed in the myocardium (Fig. 2E,H,Z). $Ca_{v1.3}$ expression is noticeably weaker than $Ca_{v1.2}$ and $Ca_{v3.2}$ at this stage and appears to diminish toward swimming tadpole stages (Figs. 2H,I, 3C). $Ca_{v1.2}$ and $Ca_{v3.2}$ expression, on the other hand, appears to strengthen as development progresses (Figs. 2F,F',AA, 3B, 4J).

Fig. 6. Spinal cord histological analysis of voltage-gated calcium channel (VGCC) $\alpha 1$ subunit expression in stages 35–37 (swimming tadpole) *Xenopus laevis* using whole-mount in situ hybridization. A–G: Transverse 18- μ m sections within the spinal cord region of the anterior–posterior axis, with dorsal to the top. **A:** $Ca_{v1.1}$ expression. **B:** $Ca_{v1.2}$ expression. **C:** $Ca_{v1.3}$ expression. **D:** $Ca_{v2.1}$ expression. **E:** $Ca_{v2.2}$ expression. **F:** $Ca_{v3.1}$ expression. **G,H:** $Ca_{v3.2}$ expression. Arrowheads indicate regions of expression. Abbreviations: sc, spinal cord; so, somite. Scale bar = 0.25 mm.

Fig. 7. Retina histological analysis of voltage-gated calcium channel (VGCC) $\alpha 1$ subunit expression in stage 40 (swimming tadpole) *X. laevis* using whole-mount in situ hybridization. A–G: Transverse 18- μ m sections of the retina, with dorsal to the top. **A:** $Ca_{v1.2}$ expression. **B:** $Ca_{v1.3}$ expression. **C:** $Ca_{v1.4}$ expression. **D:** $Ca_{v2.1}$ expression. **E:** $Ca_{v2.2}$ expression. **F:** $Ca_{v3.1}$ expression. **G:** $Ca_{v3.2}$ expression. Brackets indicate retinal layers with expression. GCL, ganglion cell layer; INL, inner nuclear layer; L, lens; PR, photoreceptor cells. Scale bar = 0.1 mm.

Non-neural Expression of *Ca_v1.1*

Unlike the other eight $\alpha 1$ subunits, neither *Ca_v1.1* nor *Ca_v3.3* mRNA is detected in the *X. laevis* CNS through swimming tadpole stages of development. Using in situ hybridization, *Ca_v1.1* transcripts are first observed in the somites during neurula stages (Fig. 1A,A') and continue to be expressed in the somatic and skeletal muscle tissue through swimming tadpole stages (Figs. 2A–C, 5A, 6A). By this stage of development, *Ca_v1.1* mRNA is also present in the pharyngeal arches (Figs. 2C, 3A). *Ca_v3.3* expression, on the other hand, is not observed at levels detectable using in situ hybridization in developing *X. laevis* embryos through swimming tadpole stages (data not shown).

DISCUSSION

Although most of the VGCC $\alpha 1$ subunits are expressed predominantly in the CNS, they all display remarkable diversity in their unique patterns of expression. Even those that appear similar show subtle differences temporally and spatially. For example, whole-mount in situ hybridization shows the expression of *Ca_v2.2* and *Ca_v2.1* to be nearly identical throughout development, but *Ca_v2.2* transcripts appear in the telencephalon by late tail bud stages, slightly earlier than *Ca_v2.1*. Differences are also observed between genes within specific regions where two or more are expressed. For example, *Ca_v2.1* mRNA is detected in the mid- and hindbrain in a domain that extends farther dorsally than *Ca_v1.2*, while *Ca_v3.1* and *Ca_v3.2* transcripts appear in more discrete regions of the brain and spinal cord contained within the expression realms of *Ca_v1.2*, *Ca_v1.3*, *Ca_v2.1*, and *Ca_v2.2*. This variability in expression among the various $\alpha 1$ subunits suggests that each is serving a distinct function within the developing *X. laevis* embryo. While there are no other detailed, comprehensive studies of VGCC $\alpha 1$ subunits in the vertebrate embryo, several reports have focused on subunit expression (Table 1) and calcium activity during early development. In zebrafish, *Ca_v1.1* and *Ca_v1.3* mRNA is observed

beginning at the two-cell stage and becomes restricted to the somites and CNS, respectively, later in development (Sanhueza et al., 2009). *Ca_v2.1*, *Ca_v3.1*, and *Ca_v3.2* transcripts are also detected during zebrafish gastrula stages using whole-embryo RT-PCR. In *X. laevis*, Palma et al. initially detect *Ca_v1.1* transcripts at blastula stages using whole-embryo RT-PCR. Using in situ hybridization, they observe *Ca_v1.1* mRNA in the dorsal mesoderm at gastrula stages, where it is implicated in the dorsalization of the embryo, and in the somites at neurula stages (Palma et al., 2001). An additional study has detected an L-type calcium channel in ectodermal cells in the gastrulating *Pleurodeles waltl* through labeling with a fluorescent derivative of dihydropyridine (Leclerc et al., 1995). A study by Baccaglini and Spitzer demonstrated the importance of calcium-regulated action potentials in Rohon-Beard cells of the developing *Xenopus* spinal cord (Baccaglini and Spitzer, 1977); however, no VGCC $\alpha 1$ subunit transcripts were detected in this region.

The discrepancies between these studies and the results presented here may be due to interspecies differences or variations in detection method, probe composition, or stringency of hybridization conditions. To preclude results due to cross-hybridization, our probes were designed to ensure specificity. BLAST N searches for each $\alpha 1$ subunit clone yielded only a single hit for a unique scaffold in the *X. tropicalis* genome with E values of 0.0. This suggests that cross-hybridization of specific $\alpha 1$ subunit RNA probes with other $\alpha 1$ transcripts during high-stringency in situ hybridization in this study is unlikely, a result supported by the unique expression patterns for each subunit.

Other descriptions of $\alpha 1$ subunit embryonic expression have focused on specific areas of organogenesis at later stages of vertebrate development (Table 1). Using pharmacological and electrophysiological approaches on culture neurons, Li et al. (2001) and Thaler et al. (2001) have shown N, L, R, and even T-type channels are present in the *Xenopus* spinal cord, specifically at the neuromuscular junction. Localization of

Ca_v3.2 mRNA in the mouse brain at embryonic day (E) 9 and subsequent expansion into the spinal cord and heart by E12 is spatially consistent with *X. laevis* expression (Son et al., 2002). *Ca_v3.2* has also been shown, in agreement with *X. laevis* expression, to be the major T-type $\alpha 1$ subunit expressed in E9.5 mice before becoming superseded by *Ca_v3.1* expression by E18 (Niwa et al., 2004). A contrasting study, however, finds *Ca_v3.2* is expressed at lower levels than *Ca_v1.2*, *Ca_v1.3*, *Ca_v1.1*, and especially *Ca_v3.1* from E9.5 to E15.5 (Xu et al., 2003). Lastly, expression of *Ca_v1.2*, *Ca_v1.3*, and *Ca_v3.1* is detected in E8 cochlear chick hair cells; with the exception of *Ca_v1.2*, these findings are consistent with *X. laevis* expression data (Levic et al., 2007).

The expression patterns of the auxiliary VGCC β subunits are much more thoroughly described in early vertebrate embryonic development, particularly in zebrafish. Isoforms for the $\beta 2$ and $\beta 4$ subunits are detected at the four-cell stage (Ebert et al., 2008a,b), and spatial expression analysis of isoforms for $\beta 1$, $\beta 2$, $\beta 3$, and $\beta 4$ detects these subunits primarily in the skeletal muscle, the CNS, and, in the case of *cacnb4a*, the heart by 72 hours postfertilization (hpf; Zhou et al., 2006,2008). Each type has at least one isoform that is expressed in the brain, spinal cord, retina, trigeminal ganglion, and spinal cord, suggesting regions of potential coexpression and association with most of the $\alpha 1$ subunits based on *X. laevis* expression patterns. Other expression domains, such as $\beta 2$ in the retinal photoreceptor cells or $\beta 3$ in otic cells, show that, while overlap exists outside the brain and spinal cord, no β subunit expression pattern perfectly matches with any *X. laevis* $\alpha 1$ subunit. For example, zebrafish *cacnb1* is the only β subunit to be expressed in skeletal muscle (Zhou et al., 2006), like *X. laevis* *Ca_v1.1*, but it is also located throughout the CNS, indicating that, if it is functioning as an auxiliary VGCC subunit, it could be associating with more than one $\alpha 1$ subtype. Interestingly, while zebrafish studies identify *cacnb1* as the only β subunit to appear in skeletal muscle (Zhou et al., 2006, 2008),

TABLE 1. Summary of Embryonic and Adult Vertebrate CACNA Expression Patterns^a

Gene	Embryonic Vertebrate Expression ^b	Stage of Onset ^b	Adult Vertebrate Expression
<i>CACNA1S</i>	<i>Widespread</i> ¹	<i>2-cell (zebrafish)</i>	Skeletal muscle ⁷
<i>Cav1.1</i>	<i>Dorsal mesoderm</i> ²	<i>Gastrula (X. laevis)</i>	
L-type	Dorsal mesoderm/somites ^{1,2}	Neurula	
	Pharyngeal arches	Swimming tadpole	
<i>CACNA1C</i>	Neural tube/spinal cord, CN VII	Neurula	Brain (cortex, hippocampus, cerebellum) ^{8,9} , spinal cord motoneurons ^{10,11} , retina (IPL, INL, OPL) ^{12,13} , heart ⁷ , smooth muscle (blood vessels, intestine, lung, uterus)
<i>Cav1.2</i>	Forebrain, midbrain, hindbrain, CN V, heart ³	Late tail bud	
L-type	Pineal gland, CN VIII, IX, X, retina (GCL, INL)	Swimming tadpole	
	<i>Cochlear hair cells</i> ⁴	<i>E8 (chick)</i>	
<i>CACNA1D</i>	Forebrain ¹	Early tail bud	Brain (cortex, hippocampus, cerebellum) ^{8,9} , spinal cord motoneurons ^{10,11} , cochlear hair cells ⁷ , retina (GCL, IPL, INL, OPL, ONL) ¹² , heart ⁷ , pancreas
<i>Cav1.3</i>	Pineal gland ¹ , midbrain ¹ , hindbrain ¹ , ventralotic vesicle ⁴ , spinal cord ¹ , retina ¹ (GCL, INL, ONL), heart ³	Late tail bud	
L-type			
<i>CACNA1F</i>	Retina (ONL)	Swimming tadpole	Retina (GCL, ONL) ¹³ , spinal cord ⁷ , lymphoid tissue
<i>Cav1.4</i>			
L-type			
<i>CACNA1A</i>	Neural tube/spinal cord, CN VII	Neurula	Brain (cortex, hippocampus, cerebellum, brainstem, olfactory bulb, thalamus) ^{9,14} , spinal cord motoneurons ^{10,15} , retina (GCL, IPL, INL, OPL) ^{12,13} , heart ⁷ , pancreas
<i>Cav2.1</i>	Hindbrain, CN V	Early tail bud	
P/Q-type	Forebrain, midbrain, retina (GCL, INL)	Late tail bud	
	Pineal gland, CN VIII, IX, X	Swimming tadpole	
<i>CACNA1B</i>	Neural tube/spinal cord, CN VII	Neurula	Brain (cortex, hippocampus, cerebellum, brainstem) ⁹ , spinal cord motoneurons ^{10,15} , retina (GCL, IPL, INL, OPL, ONL) ^{12,13}
<i>Cav2.2</i>	Hindbrain, CN V	Early tail bud	
N-type	Forebrain, midbrain	Late tail bud	
	Retina (GCL, INL), CN VIII, IX, X	Swimming tadpole	
<i>CACNA1E</i>	Spinal cord (transient)	Early tail bud	Brain (cortex, hippocampus, cerebellum, brainstem, olfactory bulb, thalamus) ^{9,14} , spinal cord motoneurons ^{10,16} , retina (GCL, IPL, INL, ONL) ^{12,13} , heart ⁷ , testes
<i>Cav2.3</i>	Hindbrain (transient)	Late tail bud	
R-type			
<i>CACNA1G</i>	Pineal gland, hindbrain, ventral otic vesicle ⁴ , spinal cord	Late tail bud	Brain (cortex, hippocampus, olfactory bulb, thalamus, hypothalamus, midbrain, cerebellum, medulla) ^{7,17} , spinal cord motoneurons ¹⁷ , ventral cochlear nucleus, dorsal cochlear nucleus, retina (GCL, INL, OPL) ¹³ , heart ⁷ , ovary
<i>Cav3.1</i>	Forebrain, olfactory epithelium, midbrain, CN VII, retina (GCL, INL), heart ^{3,5}	Swimming tadpole	
T-type			
<i>CACNA1H</i>	Neural tube/spinal cord ⁶	Neurula	Brain (cortex, hippocampus, olfactory bulb, thalamus, hypothalamus, midbrain) ^{7,17} , spinal cord motoneurons ¹⁷ , dorsal cochlear nucleus, retina (GCL, INL, OPL) ¹³ , heart ⁷ , smooth muscle, liver, kidney
<i>Cav3.2</i>	Forebrain ⁶ , midbrain ⁶ , hindbrain ⁶ , heart ^{3,6}	Late tail bud	
T-type	Olfactory epithelium ⁶ , retina (GCL, INL), tail	Swimming tadpole	
<i>CACNA1I</i>	No expression detected	N/A	Brain (cortex, hippocampus, olfactory bulb, thalamus, hypothalamus, midbrain, cerebellum, medulla) ^{7,17} , dorsal cochlear nucleus ¹⁷ , retina (INL, OPL) ¹³
<i>Cav3.3</i>			
T-type			

^aBased on studies in mouse, rat, human, turtle, zebrafish, chick, and *X. laevis*. References: ¹Sanhuesa et al., 2009; ²Palma et al., 2001; ³Xu et al., 2003; ⁴Levic et al., 2007; ⁵Niwa et al., 2004; ⁶Son et al., 2002; ⁷Catterall et al., 2005; ⁸Hell et al., 1993; ⁹Plant et al., 1998; ¹⁰Westenbroek et al., 1998; ¹¹Simon et al., 2003; ¹²Xu et al., 2002; ¹³Witkovsky et al., 2006; ¹⁴Meacham et al., 2003; ¹⁵Aguilar et al., 2004; ¹⁶Castro et al., 2009; ¹⁷Talley et al., 1999.

^bItalics in these columns indicate expression patterns not observed in this study.

transcripts for a completely different subtype, $\beta 3$, are located in somites during early *X. laevis* development (Palma et al., 2001). Finally, there are some areas of β subunit expression, such as the $\beta 3$ -expressing spinal cord Rohon-Beard neurons, that do not appear to show $\alpha 1$ subunit expression in *X. laevis* embryogenesis (Zhou et al., 2006). This lack of complete overlap between any $\alpha 1$ - β subunit pair indicates different associations between the various $\alpha 1$ subunits and their auxiliary β subunits could be a source of Ca^{2+} activity regulation during embryogenesis. Considering the high concentration of $\alpha 1$ and β subunits in the developing nervous system, this source of regulation could be particularly important in neural development and contribute to temporal and spatial specificity in the wide range of roles Ca^{2+} signaling has been suggested to play therein.

In addition to embryonic functions, VGCCs clearly play a key role in the regulation of intercellular Ca^{2+} concentration and activity in excitable cells of the adult. Many of the expression patterns of specific VGCC $\alpha 1$ subunits we observe correlate with those reported in the adult vertebrate (Table 1). For example, *Ca_v1.1* expression in the *X. laevis* somites is consistent with the skeletal muscle expression detected in adult mammals (Catterall et al., 2005); the predominant outer nuclear layer retinal expression of *Ca_v1.4* in adult vertebrates is likewise detected in *X. laevis*; and broad neural expression of *Ca_v1.2*, *Ca_v1.3*, *Ca_v2.1*, *Ca_v2.2*, *Ca_v3.1*, and *Ca_v3.2* is observed in both vertebrate adults and *X. laevis* embryos. Nevertheless, some adult domains of expression are not present embryonically. Neither the adult neural expression of *Ca_v3.3* nor the adult cardiac expression of *Ca_v3.1* is detected in *X. laevis* through swimming tadpole stages of development, indicating these VCGGs are not involved in the embryonic development of their respective tissues. More important, however, are those patterns of embryonic expression that are not observed in the adult, such as the embryonic expression of *Ca_v2.3*, which appears to be precisely regulated spatially and temporally in a way that does not reflect its broad

neural adult expression, suggesting it is playing a role during the formation of the nervous system that differs from its adult function.

The diverse array of unique expression patterns for several of the VGCC $\alpha 1$ subunits during *X. laevis* embryonic development suggests these may be playing important roles in the formation of adult structures that are distinct from their adult functions. Several embryonic functions of Ca^{2+} signaling, such as axis formation and patterning (Palma et al., 2001; Wallingford et al., 2001), neural induction (Leclerc et al., 2006; Webb and Miller, 2006; Moreau et al., 2008), and neurotransmitter phenotype specification (Borodinsky et al., 2004; Spitzer, 2006; Root et al., 2008), have in fact been suggested. The presentation of a full overview and analysis of the embryonic expression patterns of the $\alpha 1$ subunits that control this signaling is a crucial step in defining how these processes may be mediating various aspects of embryonic development.

EXPERIMENTAL PROCEDURES

Animal Use

Embryos were obtained by means of natural matings induced with human chorionic gonadotropin as described (Mills et al., 1999; Sive et al., 2000). Staging of embryos was performed according to Nieuwkoop and Faber (1994). All procedures were performed in accordance with a protocol approved by the Institutional Animal Care and Use Committee at the College of William and Mary.

Cloning and Sequence Analysis

Primers for RT-PCR were designed from genomic sequences of *X. tropicalis* VGCC $\alpha 1$ subunits. Sequences were obtained from the genome project database of the Joint Genome Institute (transcript ID numbers: *Ca_v1.1*, 186038; *Ca_v1.2*, 365832; *Ca_v1.3*, 425287; *Ca_v1.4*, 470861; *Ca_v2.1*, 470594; *Ca_v2.2*, 189681; *Ca_v2.3*, 467646; *Ca_v3.1*, 380951; *Ca_v3.2*, 311573; *Ca_v3.3*, 323418) through BLAST N searches using mouse and human orthologs. Primer

pairs for each channel were selected from regions that were unique to that particular channel (to ensure that a specific channel would be cloned) but highly conserved among species (to ensure that the primers would recognize *X. laevis* sequences). Primers used for the cloning were as follows: *Ca_v1.1*, (5'-AACCGCTTTGACTGCTT TGT-3'), and (5'-GTTCTTGTCCAGC TCACAGTT-3'); *Ca_v1.2*, (5'-GCCTGT GGAAGTTATCGAA-3'), and (5'-TT GCTCTGTTGACCCGTAA-3'); *Ca_v1.3*, (5'-TTCCTCATCCCCCTCTTCT-3'), and (5'-ATCGATGCTGCAAGGCA AG-3'); *Ca_v1.4*, (5'-GCCTGCATC AGCATTGTAGA-3'), and (5'-TTCTC CCTCAGCTTTTGAA-3'); *Ca_v2.1*, (5'-GGAGAGCCAGTCTTGGATGA-3'), and (5'-AGTAACCATTTGGGCAACCT G-3'); *Ca_v2.2*, (5'-GGGATGAACGTCC AGAATTG-3'), and (5'-GCGCTTCTA CTCCTGTGACC-3'); *Ca_v2.3*, (5'-TATT TCATTGGGATATTTTGCTTTG-3'), and (5'-GACGTGGACCCATTCCATA C-3'); *Ca_v3.1*, (5'-ATCCTCCTCAACT GCGTGAC-3'), and (5'-CCCATGCTG AGGGTGTATTAT-3'); *Ca_v3.2*, (5'-CCC ACCGTCTTCTTCTGTCT-3'), and (5'-TGATACTCAATCCCATGCTC-3'); *Ca_v3.3*, (5'-CCTTCATCTTCTCAACT GC-3'), and (5'-AAGTTCTCAACCAC GACACC-3').

Total RNA was extracted from stage 40 *X. laevis* embryos using the RNeasy Maxi kit (Qiagen), and cDNA was synthesized using the iScript cDNA Synthesis kit (Bio-Rad) following manufacturers' instructions. PCR was performed using either *Taq* DNA polymerase (New England Biolabs) or the Supertaq DNA Polymerase kit (Ambion). PCR products were cloned into the pCRII-TOPO vector and transformed into One Shot DH5 α Chemically Competent *Escherichia coli* (Invitrogen) or into the StrataClone pSC-A-amp/kan vector and transformed using StrataClone Solo-Pack Competent Cells (Stratagene). Plasmid DNA containing the cloned PCR products was purified using the Wizard Plus SV Miniprep Kit (Promega) and sequenced on an ABI 3130 Genetic Analyzer sequencer using the BigDye Terminator v3.1 Ready Reaction Cycle Sequencing Kit (Applied Biosystems). The identity of each clone was verified by nucleotide and deduced amino acid BLAST comparisons with orthologous sequences from

a range of organisms including *X. tropicalis*.

Expression Analysis

Antisense mRNA probes were generated for each of the $\alpha 1$ subunits by linearizing the plasmid DNA with a restriction enzyme and transcribing with an RNA polymerase as follows: *Ca_v1.1* (*EcoRV*, Sp6); *Ca_v1.2* (*NotI*, T3); *Ca_v1.3* (*NotI*, T3); *Ca_v1.4* (*NotI*, T3); *Ca_v2.1* (*BamHI*, T3); *Ca_v2.2* (*Hind III*, T7); *Ca_v2.3* (*EcoRV*, Sp6); *Ca_v3.1* (*NotI*, T3); *Ca_v3.2* (*NotI*, T3); *Ca_v3.3* (*EcoRV*, Sp6). High stringency whole-mount in situ hybridization analysis using NBT/BCIP (nitroblue tetrazolium/5-bromo-4-chloro-3-indolyl phosphate) alkaline phosphatase substrate (Promega) was carried out as described with minor modifications (Harland, 1991). Sense probes were used to exclude the possibility of non-specific hybridization.

Following whole-mount in situ hybridization, embryos were dehydrated and cleared as described for whole-mount photography (Sive et al., 2000). For histological analysis, embryos were cryoprotected in 1.6 M sucrose in phosphate buffered saline for at least 12 hr at 4°C, embedded in Tissue Freezing Medium at -20°C, cryosectioned into 18 μ m slices, and mounted on slides for photography. Histological analysis of embryos from Figure 1 was performed as previously described (Li et al., 2006).

ACKNOWLEDGMENTS

We thank Lomax Boyd for his suggestions on the manuscript. Support was provided by a grant from the Howard Hughes Medical Institute Undergraduate Science Education Program to the College of William and Mary and from the NIH (R15NS067566).

REFERENCES

Aguilar J, Escobedo L, Bautista W, Felix R, Delgado-Lezama R. 2004. N- and P/Q-type Ca²⁺ channels regulate synaptic efficacy between spinal dorsolateral funicular terminals and motoneurons. *Biochem Biophys Res Commun* 317: 551–557.

Baccaglioni PI, Spitzer NC. 1977. Developmental changes in the inward current of the action potential of Rohon-Beard neurones. *J Physiol* 271:93–117.

Borodinsky LN, Spitzer NC. 2006. Second messenger pas de deux: the coordinated dance between calcium and cAMP. *Sci STKE*2006:pe22.

Borodinsky LN, Root CM, Cronin JA, Sann SB, Gu X, Spitzer NC. 2004. Activity-dependent homeostatic specification of transmitter expression in embryonic neurons. *Nature* 429: 523–530.

Calin-Jageman I, Lee A. 2008. Ca(v)1 L-type Ca²⁺ channel signaling complexes in neurons. *J Neurochem* 105:573–583.

Castro A, Andrade A, Vergara P, Segovia J, Aguilar J, Felix R, Delgado-Lezama R. 2009. Involvement of R-type Ca²⁺ channels in neurotransmitter release from spinal dorsolateral funicular terminals synapsing motoneurons. *J Comp Neurol* 513:188–196.

Catterall WA. 2000. Structure and regulation of voltage-gated Ca²⁺ channels. *Annu Rev Cell Dev Biol* 16:521–555.

Catterall WA, Perez-Reyes E, Snutch TP, Striessnig J. 2005. International Union of Pharmacology. XLVIII. Nomenclature and structure-function relationships of voltage-gated calcium channels. *Pharmacol Rev* 57:411–425.

Conklin MW, Lin MS, Spitzer NC. 2005. Local calcium transients contribute to disappearance of pFAK, focal complex removal and deadhesion of neuronal growth cones and fibroblasts. *Dev Biol* 287:201–212.

Ebert A, McAnelly C, Srinivasan A, Mueller R, Garrity D. 2008a. The calcium channel beta2 (CACNB2) subunit repertoire in teleosts. *BMC Mol Biol* 9:38.

Ebert AM, McAnelly CA, Srinivasan A, Linker JL, Horne WA, Garrity DM. 2008b. Ca²⁺ channel-independent requirement for MAGUK family CACNB4 genes in initiation of zebrafish epiboly. *Proc Natl Acad Sci U S A* 105:198–203.

Harland RM. 1991. In situ hybridization: an improved whole-mount method for *Xenopus* embryos. *Methods Cell Biol* 36:685–695.

Hell JW, Westenbroek RE, Warner C, Ahljianian MK, Prystay W, Gilbert MM, Snutch TP, Catterall WA. 1993. Identification and differential subcellular localization of the neuronal class C and class D L-type calcium channel alpha 1 subunits. *J Cell Biol* 123:949–962.

Horner VL, Wolfner MF. 2008. Transitioning from egg to embryo: triggers and mechanisms of egg activation. *Dev Dyn* 237:527–544.

Jimenez-Gonzalez C, McLaren GJ, Dale N. 2003. Development of the Ca²⁺-channel and BK-channel expression in embryos and larvae of *Xenopus laevis*. *Eur J Neurosci* 18:2175–2187.

Kisilevsky AE, Zamponi GW. 2008. Presynaptic calcium channels: structure, regulators, and blockers. *Handb Exp Pharmacol*:45–75.

Leclerc C, Duprat AM, Moreau M. 1995. In vivo labelling of L-type Ca²⁺ channels by fluorescent dihydropyridine: correlation between ontogenesis of the channels and the acquisition of neural competence in ectoderm cells from *Pleurodeles waltl* embryos. *Cell Calcium* 17: 216–224.

Leclerc C, Neant I, Webb SE, Miller AL, Moreau M. 2006. Calcium transients and calcium signalling during early neurogenesis in the amphibian embryo *Xenopus laevis*. *Biochim Biophys Acta* 1763:1184–1191.

Levic S, Nie L, Tuteja D, Harvey M, Sokolowski BHA, Yamoah EN. 2007. Development and regeneration of hair cells share common functional features. *Proc Natl Acad Sci U S A* 104: 19108–19113.

Li W, Thaler C, Brehm P. 2001. Calcium channels in *Xenopus* spinal neurons differ in somas and presynaptic terminals. *J Neurophysiol* 86:269–279.

Li M, Sipe CW, Hoke K, August LL, Wright MA, Saha MS. 2006. The role of early lineage in GABAergic and glutamatergic cell fate determination in *Xenopus laevis*. *J Comp Neurol* 495:645–657.

Li WM, Webb SE, Chan CM, Miller AL. 2008. Multiple roles of the furrow deepening Ca²⁺ transient during cytokinesis in *Zebrafish* embryos. *Dev Biol* 316: 228–248.

McKeown L, Robinson P, Jones OT. 2006. Molecular basis of inherited calcium channelopathies: role of mutations in pore-forming subunits. *Acta Pharmacol Sin* 27:799–812.

Meacham CA, White LD, Barone S, Shaffer TJ. 2003. Ontogeny of voltage-sensitive calcium channel alpha(1A) and alpha(1E) subunit expression and synaptic function in rat central nervous system. *Brain Res Dev Brain Res* 142: 47–65.

Mills KR, Kruep D, Saha MS. 1999. Elucidating the origins of the vascular system: a fate map of the vascular endothelial and red blood cell lineages in *Xenopus laevis*. *Dev Biol* 209: 352–368.

Moreau M, Neant I, Webb SE, Miller AL, Leclerc C. 2008. Calcium signalling during neural induction in *Xenopus laevis* embryos. *Philos Trans R Soc Lond B Biol Sci* 363:1371–1375.

Nieuwkoop PD, Faber J. 1994. Normal table of *Xenopus laevis* (Daudin). New York: Garland Publishing.

Niwa N, Yasui K, Opthof T, Takemura H, Shimizu A, Horiba M, Lee J-K, Honjo H, Kamiya K, Kodama I. 2004. Cav3.2 subunit underlies the functional T-type Ca²⁺ channel in murine hearts during the embryonic period. *Am J Physiol Heart Circ Physiol* 286:H2257–H2263.

Obermair GJ, Tuluc P, Flucher BE. 2008. Auxiliary Ca(2+) channel subunits: lessons learned from muscle. *Curr Opin Pharmacol* 8:311–318.

Palma V, Kukuljan M, Mayor R. 2001. Calcium mediates dorsoventral patterning of mesoderm in *Xenopus*. *Curr Biol* 11:1606–1610.

Perez-Reyes E, Schneider T. 1995. Molecular biology of calcium channels. *Kidney Int* 48:1111–1124.

- Plant TD, Schirra C, Katz E, Uchitel OD, Konnerth A. 1998. Single-cell RT-PCR and functional characterization of Ca²⁺ channels in motoneurons of the rat facial nucleus. *J Neurosci* 18:9573–9584.
- Root CM, Velazquez-Ulloa NA, Monsalve GC, Minakova E, Spitzer NC, Ribera AB. 2008. Embryonically expressed GABA and glutamate drive electrical activity regulating neurotransmitter specification. *J Neurosci* 28:4777–4784.
- Sanhueza D, Montoya A, Sierralta J, Kukuljan M. 2009. Expression of voltage-activated calcium channels in the early zebrafish embryo. *Zygote* 17: 131–135.
- Simon M, Perrier JF, Hounsgaard J. 2003. Subcellular distribution of L-type Ca²⁺ channels responsible for plateau potentials in motoneurons from the lumbar spinal cord of the turtle. *Eur J Neurosci* 18:258–266.
- Sive HL, Grainger RM, Harland RM. 2000. Early development of *Xenopus laevis*: a laboratory manual. Cold Spring Harbor, NY: Cold Spring Harbor Laboratory Press.
- Son WY, Han CT, Lee JH, Jung KY, Lee HM, Choo YK. 2002. Developmental expression patterns of alpha1H T-type Ca²⁺ channels during spermatogenesis and organogenesis in mice. *Dev Growth Differ* 44:181–190.
- Spitzer NC, Ribera AB. 1998. Development of electrical excitability in embryonic neurons: mechanisms and roles. *J Neurobiol* 37:190–197.
- Spitzer NC. 2006. Electrical activity in early neuronal development. *Nature* 444:707–712.
- Spitzer NC, Kingston PA, Manning TJ, Conklin MW. 2002. Outside and in: development of neuronal excitability. *Curr Opin Neurobiol* 12:315–323.
- Spitzer NC, Borodinsky LN, Root CM. 2005. Homeostatic activity-dependent paradigm for neurotransmitter specification. *Cell Calcium* 37:417–423.
- Talley EM, Cribbs LL, Lee J, Daud A, Perez-Reyes E, Bayliss DA. 1999. Differential distribution of three members of a gene family encoding low voltage-activated (T-type) calcium channels. *J Neurosci* 19:1895–1911.
- Thaler C, Li W, Brehm P. 2001. Calcium channel isoforms underlying synaptic transmission at embryonic *Xenopus* neuromuscular junctions. *J Neurosci* 21:412–422.
- Wallingford JB, Ewald AJ, Harland RM, Fraser SE. 2001. Calcium signaling during convergent extension in *Xenopus*. *Curr Biol* 11:652–661.
- Webb SE, Miller AL. 2006. Ca²⁺ signaling and early embryonic patterning during the blastula and gastrula periods of zebrafish and *Xenopus* development. *Biochim Biophys Acta* 1763:1192–1208.
- Westenbroek RE, Hoskins L, Catterall WA. 1998. Localization of Ca²⁺ channel subtypes on rat spinal motor neurons, interneurons, and nerve terminals. *J Neurosci* 18:6319–6330.
- Witkovsky P, Shen C, McRory J. 2006. Differential distribution of voltage-gated calcium channels in dopaminergic neurons of the rat retina. *J Comp Neurol* 497:384–396.
- Xu HP, Zhao JW, Yang XL. 2002. Expression of voltage-dependent calcium channel subunits in the rat retina. *Neurosci Lett* 329:297–300.
- Xu M, Welling A, Papparisto S, Hofmann F, Klugbauer N. 2003. Enhanced expression of L-type Cav1.3 calcium channels in murine embryonic hearts from Cav1.2-deficient mice. *J Biol Chem* 278:40837–40841.
- Yamakage M, Namiki A. 2002. Calcium channels—basic aspects of their structure, function and gene encoding; anesthetic action on the channels—a review. *Can J Anaesth* 49:151–164.
- Zhou W, Saint-Amant L, Hirata H, Cui WW, Sprague SM, Kuwada JY. 2006. Non-sense mutations in the dihydropyridine receptor beta1 gene, CACNB1, paralyze zebrafish relaxed mutants. *Cell Calcium* 39:227–236.
- Zhou W, Horstick EJ, Hirata H, Kuwada JY. 2008. Identification and expression of voltage-gated calcium channel beta subunits in Zebrafish. *Dev Dyn* 237: 3842–3852.